Photocatalytic hydrogen and oxygen formation under visible light irradiation with M-doped InTaO$_4$ (M = Mn, Fe, Co, Ni and Cu) photocatalysts[☆]

Zhigang Zou [a], Jinhua Ye [b], Kazuhiro Sayama [a], Hironori Arakawa [a,*]

[a] *Photoreaction Control Research Center (PCRC), National Institute of Advanced Industrial Science and Technology (AIST),*
1-1-1 Higashi, Tsukuba, Ibaraki 305-8565, Japan
[b] *Materials Engineering Laboratory (MEL), National Institute for Materials Science (NIMS), 1-2-1 Sengen, Tsukuba, Ibaraki 305-0047, Japan*

Abstract

In$_{0.8}$M$_{0.2}$TaO$_4$ (M = Mn, Fe, Co, Ni, Cu) photocatalysts crystallize in the same crystal structure: wolframite type, monoclinic crystal structure with space group P2/c. The rate of H$_2$ evolution from an aqueous methanol solution under UV irradiation significantly changed with the variation of doping atoms, and In$_{0.8}$Ni$_{0.2}$TaO$_4$ showed the highest activity. Under visible light irradiation ($\lambda > 420$ nm), H$_2$ and O$_2$ were evolved from an aqueous methanol and silver nitrate solution, respectively, using the photocatalysts, In$_{0.8}$M$_{0.2}$TaO$_4$ (M = Mn, Fe, Co, Ni, and Cu). © 2002 Elsevier Science B.V. All rights reserved.

Keywords: Photocatalysts; Decomposition of water; Visible light irradiation

1. Introduction

Since photo-induced decomposition of water on TiO$_2$ electrodes was discovered [1], semiconductor-based photocatalysis has attracted extensive interest. Most of the investigations have focused on TiO$_2$, which shows relatively high activity and chemical stability under UV light irradiation. Therefore, there is an urgent need to develop new types of photocatalysts that can yield high activity under visible light irradiation, because the attempt is aimed at producing hydrogen of clean-energy from water utilizing solar energy [2–4]. Extensive studies have been performed to develop photocatalysts which can split water [5,6]. Yoshimura et al. [7] found that RbPb$_2$Nb$_3$O$_{10}$ of modified perovskite type had photocatalytic behavior and H$_2$ was evolved from an aqueous methanol solution under visible light irradiation. Inoue et al. [8] found that the oxide with tunnel structure had much more active than the generally used TiO$_2$ or SrTiO$_3$ for photocatalytic water splitting. Following after, Kudo et al. [9–11] showed that In$_2$O$_3$(ZnO)$_m$ and BiVO$_4$ could produce H$_2$ or O$_2$ from methanol or silver solutions under visible light irradiation.

Very recently, we found that InTaO$_4$ could evolve H$_2$ from pure water under visible light irradiation, but activity is very low [12]. InTaO$_4$ belongs to the family of the ABO$_4$ compounds with the A^{3+}B^{5+}O$_4$ wolframite structure. There are two kinds of octahedron in a unit cell, TaO$_6$ and InO$_6$. The TaO$_6$ and InO$_6$ octahedrons form the layers by sharing the corner. Oxygen planes are formed in parallel with (0 0 1) plane. We considered that M (M = Mn, Fe, Co, Ni, and Cu) doping of A^{3+} site in A^{3+}B^{5+}O$_4$ might cause a slight modification of crystal structure, resulting in a change in photocatalytic property. It is known that a slight modification of structure to semiconductor has a dramatic effect on the physical properties [13]. Here we report the synthesis, photocatalytic and structural characterizations of these new photocatalysts, In$_{0.8}$M$_{0.2}$TaO$_4$ (M = Mn, Fe, Co, Ni, and Cu). A comparison of the photocatalytic properties of the new photocatalysts with the TiO$_2$ photocatalyst is presented.

2. Experimental

Polycrystalline samples of In$_{0.8}$M$_{0.2}$TaO$_4$ (M = Mn, Fe, Co, Ni, and Cu) were synthesized by the solid-state reaction method. The pre-dried In$_2$O$_3$, Ta$_2$O$_5$, MnO$_2$, Fe$_2$O$_3$, CoO, NiO and CuO with purity of 99.99% were used as starting materials. The stoichiometric amounts of precursors were

mixed and pressed into small columns. The columns were reacted in an aluminum crucible in air for 2 days at 1100 °C.

The chemical composition of the samples before and after photocatalytic reaction was determined by scanning electron microscope–X-ray energy dispersion spectrum (SEM–EDS) with accelerating voltage of 25 kV. The crystal structure of the samples was determined by powder X-ray diffraction method using Cu Kα radiation ($\lambda = 1.54178$ Å). UV–Vis diffuse reflectance spectrum of the photocatalysts was measured by using an UV–Vis spectrometer (MPS-2000). The surface area was determined by BET measurement (Micromeritics, Shimadzu, Flow-Prep 060).

Photocatalytic reaction was carried out in a closed gas circulation system. The gases evolved were determined with TCD gas chromatograph, which was connected to a gas circulating line. In order to obtain high activity, it is essential to load a metal or metal oxide on the surface of photocatalyst. Because the addition of noble metals or metal oxides on a surface of semiconductor can change the photocatalytic properties by changing the semiconductor surface properties. The Pt was found to be the most effective for TiO_2 photocatalyst. We loaded Pt onto the catalyst surface by in situ photodeposition method in our experiments to obtain higher activity from H_2PtCl_6. Under light irradiation H_2PtCl_6 in solution is reduced to metallic state and deposited onto surface of catalyst powder, forming Pt/catalyst.

The photocatalytic reaction under UV irradiation was examined using an inner-irradiation type quartz cell with 400 W high-pressure Hg lamp and in an aqueous CH_3OH/H_2O solution (0.5 g powder catalyst, 50 ml CH_3OH, 300 ml H_2O and 0.1 wt.% Pt (Pt-loading instead of a H_2PtCl_6)). The photocatalytic reaction under visible light irradiation was examined using a Pyrex glass cell, 300 W Xe arc lamp and in an aqueous CH_3OH/H_2O solution (0.5 g powder catalyst, 50 ml CH_3OH, 200 ml H_2O and 0.1 wt.% Pt (Pt-loading instead of a H_2PtCl_6)). The 420 nm cut filter was placed onto the window face of the Pyrex glass cell. O_2 evolution reaction was performed in an aqueous silver nitrate solution (0.5 g powder catalyst, 0.5 mmol $AgNO_3$, 250 ml H_2O) under visible light irradiation ($\lambda > 420$ nm).

3. Results and discussion

The chemical composition of the photocatalysts before and after photocatalytic reaction was determined using characteristic X-rays of M Lα (M = In, Mn, Fe, Co, Ni, and Cu) and Ta Lα. The composition content was determined using the *ZAF* (*Z*: element number ("Z" number) correction; *A*: absorption correction; *F*: fluorescence correction) quantification method. The SEM–EDS analysis showed that the photocatalysts have a homogenous atomic distribution with no other additional elements. The chemical composition of these samples after reaction is also same with that of samples before reaction.
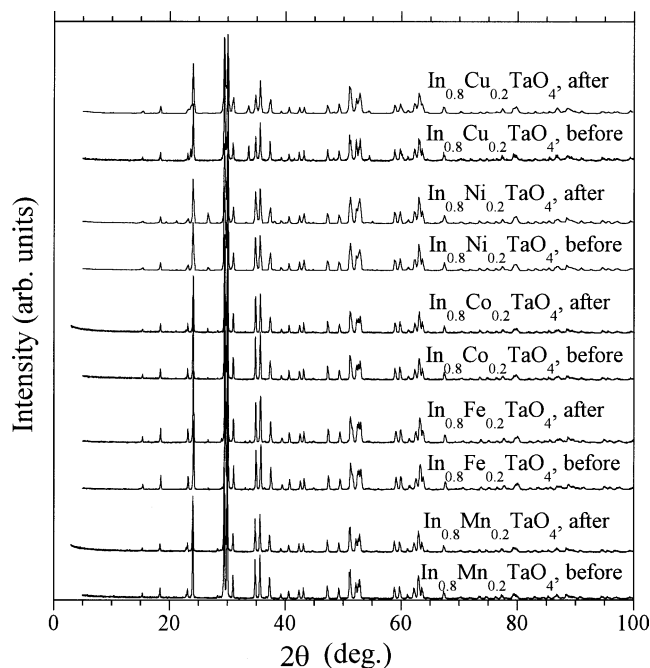

Fig. 1. X-ray powder diffraction patterns of photocatalysts before and after photocatalytic reaction.

The crystal structure of the photocatalysts before and after photocatalytic reactions was investigated using X-ray powder diffraction. The result is shown in Fig. 1. The data were collected at 295 K with a step scan procedure in the range of $2\theta = 5$–$100°$. The step interval was $0.024°$ and scan speed, $1°$ min^{-1}. The powder X-ray diffraction analysis showed that all samples are the single phases. We can see that the Bragg peak distributions of the photocatalysts remain unchanged, indicating that the photocatalysts crystallize in the same crystal structure. Full-profile structure refinement of the collected powder diffraction data was performed using the Rietveld program REITAN [14]. Positional parameters and isotropic thermal parameters of the photocatalysts were refined. The result of refinement shows all the photocatalysts crystallize in the same wolframite structural type, monoclinic with space group P2/c.

The $InTaO_4$ photocatalyst has two kinds of octahedron in a unit cell, TaO_6 and InO_6 [12]. The volume of InO_6 octahedron in $InTaO_4$ is 13.601 Å^3. However, the volume of TaO_6 is 10.648 Å^3. This means that the volume of InO_6 octahedron was changed when In is doped by M (M = Mn, Fe, Co, Ni, and Cu) because the change of the M atomic radius, but crystal structure could not change. The change of the InO_6 volume leads to a slight change of the lattice parameters in the doped-$InTaO_4$ system. The details of the investigation on structure was published elsewhere [15]. We confirmed that the photocatalysts have changed neither the crystal structure nor the chemical composition after photocatalytic reaction.

Table 1 summarizes the H_2 evolution rate under UV and visible light irradiation, respectively, and catalyst

Table 1
Rates of gas evolution and physical properties of the photocatalysts

Photocatalyst[a]	Surface area (m^2/g)	Rate of evolution ($\mu mol\,h^{-1}$)			
		UV irradiation[b], CH_3OH/H_2O		Visible light irradiation[c], $\lambda > 420\,nm$	
		H_2	CO	CH_3OH/H_2O, H_2	$AgNO_3/H_2O$, CO
$InTaO_4$[d]	1.35	270	15	1.2	0.8
$In_{0.8}Mn_{0.2}TaO_4$	0.95	310	25	0.5	0.3
$In_{0.8}Fe_{0.2}TaO_4$	0.82	80	4	Non-doped	Non-doped
$In_{0.8}Co_{0.2}TaO_4$	0.93	370	35	0.6	0.6
$In_{0.8}Ni_{0.2}TaO_4$	0.97	470	45	3.1	1.1
$In_{0.8}Cu_{0.2}TaO_4$	0.81	100	5	Non-doped	Non-doped
TiO_2 (P25)	53.8	550	15	Non-doped	Non-doped

[a] Pt (0.1 wt.%) was loaded on the surface of powder catalyst.
[b] 1.0 g powder catalyst under UV irradiation using 400 W high-pressure Hg lamp.
[c] 0.5 g powder catalyst under visible light irradiation using 300 W Xe arc lamp.
[d] The quantum yield at 402 nm was estimated to be 0.33% by using an interference filter (λ: 402 nm, half width: 15.3 nm).

characterization for these photocatalysts. Our catalysts are compared with TiO_2 (P25). It is noted that TiO_2 shows very high activity under UV irradiation, but the photocatalytic activity is not observed under visible light irradiation (see Table 1). This is consistent with the bandgap of TiO_2. The bandgap of TiO_2 is 3.2 eV, which cannot respond to wavelength range of visible light. BET measurement showed that the surface areas of M-doped $InTaO_4$ are about 0.95 m^2/g as shown in Table 1. Since this is only about 2% of the surface area of the TiO_2 photocatalyst (see Table 1), it demonstrates the much higher efficiency of the new photocatalysts. It is evident that further increase in activity might be expected from increasing the surface area. Since an efficient photocatalytic reaction process occurs on the photocatalyst surface, the increase of the surface area for the photocatalysts might lead to the increase of their photocatalytic activity.

The photocatalytic activity significantly changed with the variation of doping atoms (M = Mn, Fe, Co, Ni, and Cu) in $InTaO_4$. Fig. 2 shows the H_2 evolution from CH_3OH/H_2O solution under UV irradiation. The formation rates of H_2 were estimated to be 0.31, 0.08, 0.37, 0.47 and 0.1 mmol h^{-1} in the first 10 h for Mn, Fe, Co, Ni and Cu, respectively. The amount of evolved H_2 (mol) exceeded the amount of catalyst (about 1.38 mmol) at 24 h, indicating that the reaction occurs catalytically. The reaction stopped when the light was turned off in this experiment, showing the obvious light response. The result shows that the photocatalytic reaction is induced by the absorption of UV irradiation. The formation rate of H_2 increased on Mn, Co and Ni-doped $InTaO_4$, but decreased on the Cu and Fe-doped $InTaO_4$ photocatalysts than that of non-doped $InTaO_4$. The formation rate of H_2 on $In_{0.8}Ni_{0.2}TaO_4$ is about 180% than that of non-doped $InTaO_4$. The CO evolution was observed in this reaction from CH_3OH/H_2O solution as the oxidation product. The result is shown in Table 1. The CO evolution increases with illumination time, as does H_2 evolution. However, the rate of CO evolutions is much lower than that of H_2 evolution. The CO is probably from decomposition of the formaldehyde, which decomposes slower than
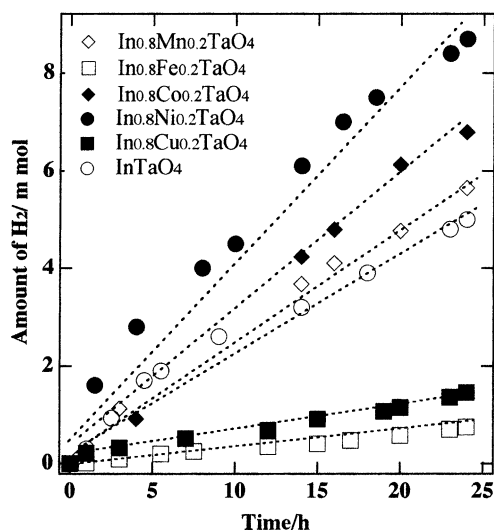

Fig. 2. Photocatalytic H_2 evolution on the $In_{0.8}M_{0.2}TaO_4$ (M = Mn, Fe, Co, Ni, and Cu) compound from CH_3OH/H_2O solution under UV irradiation.

methanol dehydrogenates. On the other hand, the ratios of non-stationary and non-stoichiometry evolutions between H_2 and CO might result from generation of CO_2 and other evolutions. It is well known that when CH_3OH is added to a Pt/TiO_2 aqueous suspension, sustained H_2 production is observed under UV irradiation and the alcohol molecules are oxidized to final productions of CO_2, CO, CH_4, etc. [20]. The presence of oxygen vacancy defects strongly enhances such interaction due to electron back-donation from surface Ti^{3+} into π^* orbital of molecular CO [20]. The formation rate of CO changed with the variation of doping atoms, showing the same tendency as observed in H_2 evolution.

Under visible light irradiation ($\lambda > 420$ nm) H_2 and O_2 were evolved using the Mn, Co and Ni-doped $InTaO_4$ photocatalysts from CH_3OH/H_2O and $AgNO_3/H_2O$ solutions, respectively. The Cu and Fe-doped $InTaO_4$ photocatalysts cannot work at same conditions. Fig. 3 shows the H_2 evolution from CH_3OH/H_2O solution under visible light
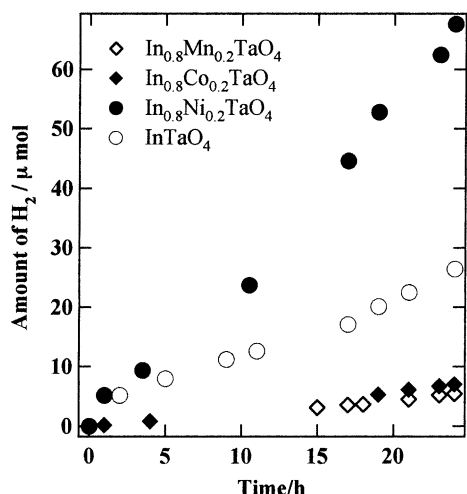
Fig. 3. Photocatalytic H_2 evolution from CH_3OH/H_2O solution under visible light irradiation, $\lambda > 420$ nm.
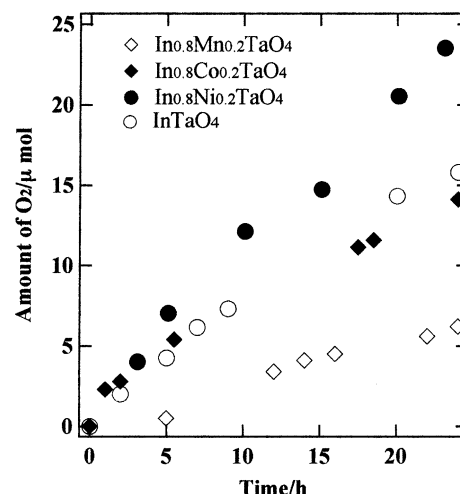

Fig. 4. Photocatalytic O_2 evolution from an aqueous silver nitrate solution under visible light irradiation, $\lambda > 420$ nm.

irradiation using Mn, Co and Ni-doped $InTaO_4$ photocatalysts. The H_2 evolution increases with illumination time. The formation rate of H_2 on Ni-doped $InTaO_4$ is much higher than that of the non-doped $InTaO_4$ photocatalyst, as does H_2 evolution under UV irradiation. The CO evolution was observed in this reaction from CH_3OH/H_2O solution as the oxidation product. However, the formation rates of H_2 on Mn and Co-doped $InTaO_4$ are much lower than that of the non-doped $InTaO_4$ photocatalyst. The effect of visible light irradiation was investigated by dark experiment. The H_2 evolution stopped when light irradiation was terminated, showing the obvious visible light response. As a typical example, we examined the quantum yielded for non-doped $InTaO_4$ photocatalyst as shown in Table 1. The quantum yield at 402 nm was estimated to be 0.33% by using an interference filter (λ: 402 nm, half width: 15.3 nm).

O_2 evolution reaction was performed in an aqueous silver nitrate solution under visible light irradiation ($\lambda > 420$ nm) and the following stoichiometric reaction takes place; $4Ag^+ + 2H_2O \rightarrow 4Ag^0 + O_2 + 4H^+$ [19]. Fig. 4 shows the O_2 evolution under visible light irradiation. This result shows that these photocatalysts have potential for O_2 evolution from aqueous solution. The rate of O_2 evolution increases with In being doped by Ni in the $InTaO_4$ photocatalyst. However, the rate of O_2 evolution decreases with In being doped by Mn and Co in the $InTaO_4$ photocatalyst, as does H_2 evolution under visible light irradiation. The rate of O_2 evolution on $In_{0.8}Ni_{0.2}TaO_4$ is 1.1 μmol h^{-1}. The activity increased by about 140% than that of non-doped $InTaO_4$ (see Table 1).

It is often observed that doping transition metals into photocatalysts such as TiO_2 decreases significantly the photocatalytic activities [16]. However, such a suppression effect by doping was not predominant in the Ni-doped $InTaO_4$ photocatalyst. The activity of Ni-doped $InTaO_4$ increased under both UV and visible light irradiation, respectively. Kudo

and Sekizawa [16] found also similar phenomenon [17]. The photocatalytic activity on Ni-doped ZnS was much higher than non-doped ZnS, while that on Cu-doped ZnS was lower [17]. Although the origin is unknown yet, the band structure of NiO has been investigated [18]. The band structure of oxides is generally defined by d-level and O 2p-level of the oxides. However, the band structure of NiO is assigned to Ni 3d^8 and Ni 3d^9 [18]. This means that the Ni 3d level in the Ni-doped $InTaO_4$ photocatalyst may form a new energy level in the band structure of $InTaO_4$. The light absorption properties of the $InTaO_4$ and $In_{0.8}Ni_{0.2}TaO_4$ photocatalysts were investigated. The onset of diffuse reflection spectra showed an obvious shift to high wavelength with In being doped by Ni in $InTaO_4$. The bandgaps of $InTaO_4$ and $In_{0.8}Ni_{0.2}TaO_4$ were estimated to be 2.6 and 2.4 eV from the diffuse reflection spectra. This means that the Ni-doped $InTaO_4$ photocatalyst can utilize a wider spectral region of light irradiation than non-doped $InTaO_4$.

The difference in the surface area of the photocatalysts can generally lead to the difference in photocatalytic activity since an efficient photocatalytic reaction process occurs on the photocatalyst surface. However, the surface area of the photocatalysts is similar as shown in Table 1. It is hard to consider that the differences in the surface area of the photocatalysts led to the differences in the photocatalytic activity. In order to make clear the origin of different photocatalytic activity between the different doping atoms, further band structure analysis seem to be necessary.

The wavelengths (λ) dependence of the photocatalytic activity under the light irradiation from full arc up to $\lambda = 550$ nm was measured using different cut-off filters. The photocatalytic reaction was examined using a Pyrex glass cell, 300 W Xe arc lamp and in an aqueous CH_3OH/H_2O solution. These results are plotted in Fig. 5. The photocatalytic activity dependence of λ of light irradiation displays a normal photocatalyst behavior, with increasing λ of light
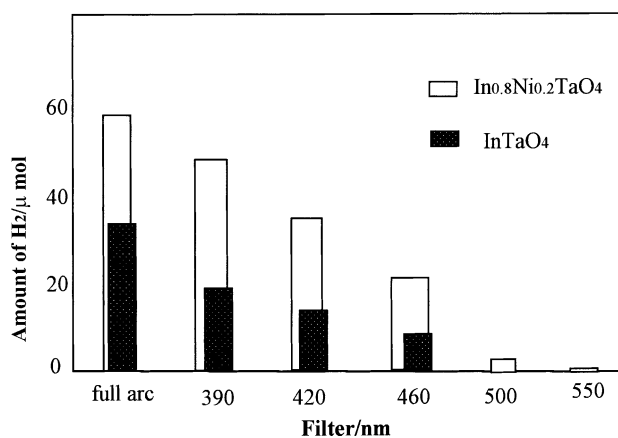
Fig. 5. The photocatalytic activity dependence of the wavelengths (λ) from full arc irradiation to $\lambda = 550$ nm; the amount of evolved H_2 at 24 h; using a Pyrex glass cell, 300 W Xe arc lamp and in an aqueous CH_3OH/H_2O solution (0.5 g powder catalyst, 50 ml CH_3OH, 200 ml H_2O and 0.1 wt.% Pt (Pt-loading instead of a H_2PtCl_6)).

irradiation, the photocatalytic activity decreases rapidly, since the number of incident photons was decreased when a cut-off filter was used. An obvious photocatalytic activity was observed when irradiated with a visible light ($\lambda > 420$ nm), showing that both $In_{0.8}Ni_{0.2}TaO_4$ and $InTaO_4$ can respond to visible light irradiation. The photocatalytic activity was also obtained when a cut-off filter of $\lambda > 460$ nm was employed. However, the activity disappeared when λ of light irradiation was larger than 500 nm. This means that light response occurred only at wavelengths shorter than 500 nm.

The process for photocatalysis of semiconductors is the direct absorption of photon by bandgap of the materials and generates electron–hole pairs in the semiconductor particles. The excitation of an electron from the valence band to the conduction band initiated by light absorption with energy equal to or greater than the bandgap of the semiconductor [4]. The diffuse reflectance spectrum of $In_{0.8}Ni_{0.2}TaO_4$ shows a visible light absorption band with the onset around 520 nm, while that of $InTaO_4$ is around 480 nm. This means that under visible light irradiation ($\lambda > 420$ nm) the Ni-doped $InTaO_4$ photocatalyst can response to range of wavelength above 40 nm than that of non-doped $InTaO_4$. The difference between the visible light absorption band of $In_{0.8}Ni_{0.2}TaO_4$ and $InTaO_4$ might led to the difference of photocatalytic activity. This is consistent with the observation of photocatalytic activity.

4. Conclusion

A new series of M-doped $InTaO_4$ (M = Mn, Fe, Co, Ni and Cu) photocatalysts were synthesized by a solid-state reaction. We have presented the evidence for photocatalytic decomposition of an aqueous solution on these photocatalysts. Our experimental results show that the photocatalysts are sensitive to UV irradiation and that it is possible to obtain H_2 from an aqueous solution. Under visible light irradiation ($\lambda > 420$ nm) H_2 and O_2 were evolved using Mn, Co and Ni-doped and non-doped $InTaO_4$ photocatalyst from CH_3OH/H_2O and $AgNO_3/H_2O$ solutions, respectively. The $In_{0.8}Ni_{0.2}TaO_4$ photocatalyst showed much higher activity than that of the non-doped $InTaO_4$ photocatalyst. Ni-doped $InTaO_4$ has been developed as a new visible light photocatalysts for H_2 and O_2 evolutions from aqueous solutions. The study of doping effects on structural and photocatalytic properties of $InTaO_4$ solid oxide photocatalyst will provide useful information on the mechanism of the photocatalysts and also on making the stable photocatalysts with high activity under visible light irradiation.

References

[1] K. Honda, A. Fujishima, Nature 238 (1972) 37.
[2] K. Tomoji, S. Tadayoshi, Nature 286 (1980) 474.
[3] B.S. Geoffrey, E.M. Thomas, J. Phys. Chem. B 101 (1997) 2508.
[4] K. Yeong, S. Samer, J.H. Munir, E.M. Thomas, J. Am. Chem. Soc. 113 (1991) 9561.
[5] Y. Kim, S. Salim, M.J. Huq, T.E. Mallouk, J. Am. Chem. Soc. 113 (1991) 9561.
[6] H.G. Kim, D.W. Hwang, J. Kim, Y.G. Kim, J. Lee, Chem. Commun. (1999) 1077.
[7] J. Yoshimure, Y. Ebina, J. Kondo, K. Domen, J. Phys. Chem. 97 (1993) 1970.
[8] Y. Inoue, Y. Asai, K. Sato, J. Chem. Soc., Faraday Trans. 90 (1994) 797.
[9] A. Kudo, I. Mikami, Chem. Lett. 1027 (1998).
[10] A. Kudo, K. Ueda, H. Kato, I. Mikami, Catal. Lett. 53 (1998) 229.
[11] A. Kudo, K. Omiori, H. Kato, J. Am. Chem. Soc. 121 (1999) 11459.
[12] Z. Zou, J. Ye, H. Arakawa, Chem. Phys. Lett. 332 (2000) 271.
[13] Z. Zou, J. Ye, K. Oka, Y. Nishihara, Phys. Rev. Lett. 80 (1998) 1074.
[14] F. Izumi, J. Crystallogr. Assoc. Jpn. 27 (1985) 23.
[15] Z. Zou, J. Ye, K. Sayama, H. Arakawa, Nature 414 (2001) 625.
[16] A. Kudo, M. Sekizawa, Chem. Comm. (2000) 1371.
[17] A. Kudo, M. Sekizawa, Catal. Lett. 58 (1999) 241.
[18] M.P. Dare-Edwards, J.B. Goodenough, A. Hamnett, N.D. Nicholson, J. Chem. Soc., Faraday Trans. II 77 (1981) 643.
[19] H. Tada, A. Hattori, Y. Tokihisa, K. Imai, N. Tohee, S. Ito, J. Phys. Chem. B 104 (2000) 4585.
[20] Z. Zou, J. Ye, R. Abe, H. Arakawa, Catal. Lett. 68 (2000) 235.